Astron. Astrophys. 346, 811–818 (1999)

ASTRONOMY AND ASTROPHYSICS

Beppo-SAX observations of AR Lacertae

M. Rodonò[1,2], I. Pagano[1,⋆], G. Leto[1,⋆⋆], F. Walter[3], S. Catalano[1], G. Cutispoto[1], and G. Umana[4]

[1] Osservatorio Astrofisico di Catania, Viale A. Doria 6, I-95125 Catania, Italy
[2] Istituto di Astronomia, Università di Catania, Viale A. Doria 6, I-95125 Catania, Italy
[3] Earth and Space Sciences Department, New York State University, Stony Brook, NY 11794-2100, USA
[4] Istituto di Radioastronomia C.N.R., Stazione VLBI, I-96017 Noto (SR), Italy

Received 4 January 1999 / Accepted 15 April 1999

Abstract. We present the results of an X-ray observation of the binary system AR Lacertae (HD 210334) obtained with the Low and Medium Energy Concentrator Spectrometers (LECS & MECS) and with the Phoswich Detector System (PDS) on board the Beppo-SAX satellite.

Two flare episodes with comparable peak luminosities were detected, one in each of the two runs into which the observations were split. Several low amplitude flares appear to be superimposed on a rotational modulated light curve. A very tight and shallow primary eclipse was observed, which is different from primary eclipses observed at other epochs by other X-ray telescopes. No sign of secondary eclipse can be inferred from these data.

The PDS data show that the emission in the 15–300 keV range is generally not detectable, but there is convincing evidence of hard photons during the onset of a flare on Nov 4 and during the flare on Nov 11. There was no significant emission in the 15–300 keV range during the major flare on Nov 4.

The AR Lac spectrum between 0.1 and 9 keV is well fit by a two component optical-thin plasma model based on the MEKAL plasma emission code with subsolar metal abundances. We also performed spectral analyses of the two separate segments of data, and found that the plasma temperatures, abundances and emission measures did not significantly change between the two time intervals.

Hints of possible H I absorption in corona or in the circumstellar enviroment are also discussed.

Key words: stars: activity – stars: binaries: general – stars: coronae – stars: individual: AR Lac – stars: late-type – stars: variables: general

1. Introduction

Thanks to their high X-ray luminosities, close binary systems were among the first stellar X-ray sources observed, and among the best studied to date. The RS CVn systems are detached close binaries with two late type stars, one of spectral type late F or G V/IV, the other of spectral type around K0 IV/III. Due to the tidal coupling of the rotational and orbital periods, all features of stellar activity that depend on rotation period are enhanced on these systems. The structure of the corona and upper transition region in RS CVn stars has been derived by fits to low resolution X-ray and EUV spectra. Swank et al. (1981) found that the *Einstein* Solid State Spectrometer (SSS) spectra could be modelled well using a two-temperature optically thin plasma. Dempsey et al. (1993) came to the same conclusion by using ROSAT PSPC data. Griffiths & Jordan (1998) showed that the two-temperature structure of coronal sources can also be inferred by an analysis of the combined EUVE and X-ray data sets, thereby casting doubt on the Majer et al. (1986) conclusion that two-temperature fits to X-ray data result from a combination of the coronal emissivities and the instrument response functions.

One of the most interesting results of recent EUV and X-ray missions (primarily EUVE and ASCA) is that some, but not all, of the most active stars appear to have coronae that are surprisingly metal poor. In fact, X-ray and EUV spectra of RS CVn and Algol binaries and of single active stars reveal metal line strengths much weaker than expected from a plasma with identical temperature/density structure but solar photospheric composition. The weak metal lines indicate a metal deficiency with respect to the solar photosphere by factors of 3 to as much as 10. Some of the sources with low coronal metal abundances also have low photospheric metal abundances (Randich et al. 1994). However, this is not a general rule, as demonstrated, e.g., by AB Dor, that is a ZAMS star with solar photospheric abundances and coronal metallicity Z$\sim$0.3 (Mewe et al. 1996). Looking at the Sun, a difference between photospheric and coronal abundances could be expected, but in the solar corona the elements with a low first ionization potential (FIP $\leq$ 10 eV) like Fe, Mg, and Si are overabundant. Güdel et al. (1999) observed on the RS CVn binary UX Ari a solar like FIP effect in the flaring coronal plasma, while the quiescent corona resulted metal poor.

AR Lacertae (HD 210334, V=6.1, d=42 pc) consists of a G2 IV primary and a K0 IV secondary star, with mass ratio $M_1/M_2 \sim 0.89$ (Marino et al. 1998), that are spin-orbit coupled with a 1.98 days period. The K star seems to be metal-deficient, but this is not the case for the G star (Naftilan & Drake 1977).

Send offprint requests to: ipagano@ct.astro.it

⋆ Visiting Member at JILA, University of Colorado, PO BOX 440, 80440 Boulder CO, USA

⋆⋆ *Present address:* CASA, University of Colorado, PO BOX 440, 80440 Boulder CO, USA

The photospheric and chromospheric activity of AR Lac have been monitored for a long time by optical photometric observations at Catania Observatory (Lanza et al. 1998) and by UV *Spectral Imaging* (Pagano et al. 1995). AR Lac is the brightest known totally eclipsing RS CVn binary. For this reason it has been one of the best observed coronal sources since the late '70s, when it was observed with the Einstein Solid State Spectrometer by Swank & White (1980). At that time its light curve in the 0.5–4 keV band did not show any evidence of eclipses. In 1980 June the *Einstein* IPC (0.1–4 keV) observed AR Lac during the eclipses and at the quadratures, covering ∼17% of the orbit (Walter et al. 1983). This X-ray light curve shows a prominent primary eclipse, as well as a shallow secondary eclipse. The rapid egress from primary minimum indicates both the small coronal scale height and the concentration of the X-ray emission toward the leading hemisphere of the G star. The shallow secondary minimum suggests an extended component around the K star. The light curve exhibits considerable structure, at the 10–20% level, outside of eclipse. In 1984 July the LEIT (0.005–2.0 keV) and ME (1.0–6.0 keV) proportional counters on EXOSAT observed a complete orbital cycle of AR Lac (White et al. 1990). Both primary and secondary eclipses were observed at low energies, but at high energies no sign of rotational modulation was found. White et al. (1990) suggested that the low temperature plasma (few times 10^6 K) was localized very close to the star in compact regions, whereas the high temperature plasma (few times 10^7 K) permeates the enviroment around the binary system and between the stars. Ottmann et al. (1993) reported on the ROSAT PSPC observations obtained in 1990 June, during the ROSAT calibration phase, which show that both the primary and the secondary eclipses were detected and that the data are compatible with a compact region (~ 0.03 $R_\odot$) close to the G star, with solar flare-like emission, plus an extended region ($\sim$ 1–2 $R_\odot$) linked to the K star, with emission resembling the solar active region emission. In 1993 June AR Lac was observed by ASCA for one complete orbit. White et al. (1994) analyzed these observations and found a 50% reduction in flux centered on the primary eclipse that was independent of energy in the 0.4–7 keV band, and a shallow minimum during the secondary eclipse. At energies $>$2 keV the ASCA light curve showed continuous low level flaring activity on a time scale of 20–60 min. White et al. (1994) found that the time-averaged X-ray spectrum in the 0.4–10 keV spectral region could be fitted by a two temperatures plasma model with metal abundances lower than solar by factors of 2–4. A similar result was found by the same authors when they analyzed a ROSAT PSPC spectrum obtained simultaneously with ASCA observations. A more detailed analysis of these ASCA/ROSAT observations was done by Kaastra et al. (1996), who confirm the results of White et al. (1994) at least qualitatively. Moreover, Siarkowski et al. (1996) used the same 1993 ASCA light curve to map the spatial structure of the AR Lac's coronae. He found that *a)* both stars are active, *b)* the X-ray emission is concentrated on the sides of the stars facing each other, *c)* there are both compact and extended coronal structures, and *d)* about 50% of the X-ray emission in unmodulated and could come from an extended halo region, from the poles of the larger K star, or from other symmetric or uneclipsed structure in the orbital plane.

As discussed by Siarkowski et al. (1996), the slow egress and long duration of the X-ray eclipses (e.g., see the SIS and GIS ASCA light curves in White et al. 1994) is one of the main clues that the coronae around both components are spatially extended. Another argument, albeit indirect, in favor of an extend corona is given by the spectral imaging analysis of the Mg II k line (Walter et al. 1987, Neff et al. 1989, Pagano 1994, Pagano et al. 1994, 1995), that revealed the existence of bright localized chromospheric regions on the K star at heights ranging from 0.3 to 1 R_* above the photosphere, suggesting the presence of extended chromospheric regions. Walter (1996) interpreted the slow egress from primary eclipse in the EUVE DS photometer (70–190 Å) light curve as due to optically thick obscuring material confined within 15° of equator of the K star and extending outward by $\sim R_K$. Such cool, dense prominence material could also be responsible for the asymetric large eclipses previously seen in the EXOSAT LE (White et al. 1990) and the ASCA light curves (White et al. 1994).

The physical interpretation of the X-ray data arising from coronal structures is greatly enhanced by simultaneous or contemporaneous data obtained at other wavelengths, to probe other aspects of the stellar atmospheres (Rodonò 1982, Linsky 1988). We had arranged for contemporaneous observations to support our SAX observations at longer wavelengths: *i)* optical photometry and H_α high dispersion spectroscopy at Catania Observatory; and *ii)* VLA and VLBA radio data from Oct 31 to Nov 4. In this paper we report on X-ray observations. The results of the optical and radio observations, as well as a complete description of the physical scenario that arises from the multiwavelength study, will be given in subsequent papers.

2. Observations and data reduction

2.1. The Beppo-SAX mission in brief

The X-ray satellite Beppo-SAX (Boella et al. 1997a) is equipped with four co-aligned Narrow Field Instruments: the measurements that we report here were obtained by using the LECS (Low Energy Concentrator Spectrometer, Parmar et al. 1997), two of the three MECS (Medium Energy Concentrator Spectrometers, Boella et al. 1997b), and the PDS Phoswich Detector System (PDS, Frontera et al. 1997). The LECS and MECS have imaging capabilities and cover the energy bands 0.1–10 keV and 1.7–10 keV, respectively. The LECS and 2 MECS instruments provide in the overlapping band an effective area that is three times the area provided by a single LECS/MECS unit, with similar energy and spectral resolution. The two instruments together allow us to study best the Fe K complex at ∼6.7 keV, which is an important diagnostic of both the coronal abundance and the temperature structure in the coronal sources. Moreover, the LECS resolution, which is comparable to the resolution of CCD detectors at low energies, and its sensitivity at energies down to 0.1 keV, where typical coronal sources have the largest X-ray flux, render the LECS data especially reliable for the study of coronal plasmas. In fact, the spectrum of a coronal source in

Table 1. Observation log of Beppo-SAX AR Lac observations on Nov 1997.

Run #	Start Day UT	End Day UT	Phase Coverage	Effective exp. time (sec) MECS	LECS	Counts MECS	LECS	Mean count rate[a] cts s^{-1} MECS	LECS	Background cts s^{-1} MECS	LECS
1	02 06:07	04 17:50	0.40–1.63	109 230	27 398	19 743	8 401	0.120±0.001	0.278±0.003	0.008± 0.007	0.006±0.006
2	11 16:14	12 15:17	0.14–0.62	44 262	20 358	7 361	6 491	0.110±0.002	0.288±0.004	0.008± 0.006	0.008±0.010

[a] Background subtracted

the region below the carbon edge (E∼0.3 keV) has few and relatively week lines and is characterized by a high signal-to-noise ratio. This relatively line-free region, as demonstrated by Favata et al. (1997a), allow us to constrain most accurately the global metallicity of the coronal plasma.

The operative energy range of the PDS is 15 to 300 keV, and this instrument can be used for both spectral and temporal studies.

2.2. The Beppo-SAX observations

The Beppo-SAX observations were obtained on 1997 Nov 2–4, and on 1997 Nov 11–12. The run Nov 11–12 was done to complete the planned observations that on Nov 4 were interrupted by a Gyro Scientific Mode (GSM) fallback during satellite orbit No. 7714. The effective exposure times are listed in Table 1. The significantly shorter-than-scheduled exposure time for the LECS instrument occured because, at the dates of observations, the LECS could be operated only during Earth dark time.

2.3. The data analysis

The data analysis was based on the linearized, cleaned event files obtained from the Beppo-SAX SDC on-line archive. Light curves and spectra were accumulated using the XSELECT Ver. 1.3 tools, using 8.5 and 4 arcmin extraction radii for the LECS and MECS, respectively, that include more than 90% of the fluxes. The resulting source counts are listed in Table 1. The background LECS and MECS spectra were extracted from the appropriate event files available from the SAX SDC public ftp site, containing the standard background observations, obtained by summing long pointings of sky regions with no detectable sources. The light curve analysis was performed using the XRONOS 5.1 package, while the spectral analysis was performed with the XSPEC 10.0 package (Arnaud 1996), implemented under FTOOLS 4.0. We used the response matrices released by the ASI SDC in September 1997. For spectral analysis, the LECS data have been analyzed only in the 0.1–4 keV range, due to still unresolved calibration problems at higher energies. We used `addspec` under FTOOLS to generate one total LECS and one total MECS spectrum by summing for each detector the two spectra observed during the two observing runs. In the following we will refer to these added spectra with the code (T). To look for short term variability of the coronal plasma, we also analyzed the two separate spectra acquired starting on Nov 2 and on Nov 11, respectively. It was not useful to further dissect the observations, mainly because the lack of LECS data during the second half of the first observing run.

The LECS and MECS spectra have been jointly fit after allowing for a rescaling of the LECS data to account for uncertainties in the intercalibration of the instruments. This rescaling factor value was determined as a free parameter of the fit. All spectra were re-binned in order to have at least 20 counts per energy bin. The background subtracted source mean count rates are given in Table 1.

3. Results

3.1. The X-ray light curves

In Fig. 1 we plot the LECS and MECS light curves binned over 360 sec. Two major flares were detected, but the first one on Nov 4 was not observed by the LECS because this instrument was not operative at that time. In the 1.7–10 keV band of the MECS, the Nov 04 flare was characterized by a rather flat maximum reached at 06:04 UT and maintained for about 1.3 h. The total energy released in this band was $\sim 6.5\times10^{34}$ erg. The second major flare was detected on Nov 11 with the flare maximum at 18:38 UT, a 1/e decay time of ∼6.4 h, and a total energy of $\sim 8.9\times10^{34}$ erg in the MECS and $\sim 1.6\times10^{35}$ erg in the LECS bandpasses, respectively. Apart from these two flares, the light curves in the range 0.1–10 keV show several minor flare-like episodes. For instance, the MECS light curve obtained during the first segment of observations, binned over 3600 sec and folded with the orbital period (see Fig. 2) shows at least five low-amplitude flares which are superimposed on the sinusoidal curve which is the best fit to the outside of eclipse and outside of flare data points drawn with filled symbols. The five low amplitude flares show increases at light maximum between 20 and 30%, values much larger than the background fluctuations as seen in Fig. 2. The sinusoidal curve can be interpreted as representative of the system X-ray quiescent emission. It indicates the presence of a well defined rotational modulation with semiamplitude ∼30%. The maximum emission occured at phase ∼0.2, indicating the presence of a bright X-ray emitting structure on the leading hemisphere of the G star or on the trailing hemisphere of the K star. As show in Fig. 2, no return to the quiescent level has followed the major flare on Nov 4, before the onset of the successive uncompletely observed flare at 15:46 UT. The data acquired during quiescence in the second observing run are not enough to see if a rotational modulated variability is still present.

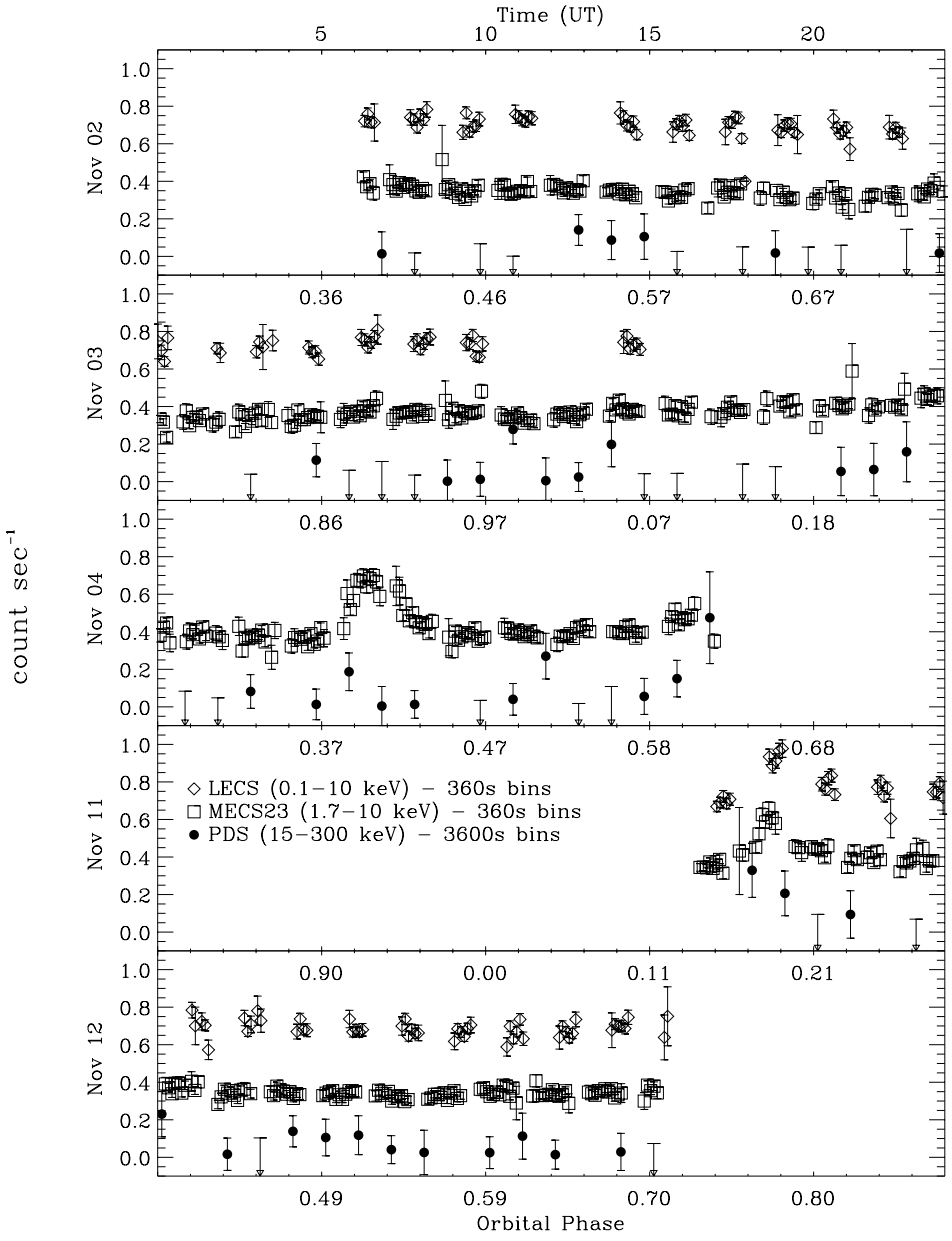

Fig. 1. SAX light curves as observed by the LECS (0.1–10 keV), MECS (1.7–10 keV) and PDS (15–300 keV) detectors. Shifts of +0.4 and +0.2 count s^{-1} were applied to the LECS and MECS count rates, respectively, to avoid the overlap of data points. Error bars indicate $\pm 1\,\sigma$ deviations. Phases label the bottom axis of each panel, and UT hours are given in the upper axis of the top panel. Phases have been computed by using the ephemeris HJD=2450692.5174+1.983188xE (Marino et al. 1998).

Our Beppo-SAX observations covered one primary eclipse, and three secondary eclipses. During the primary eclipse on Nov 3, the LECS was not operative. The MECS count rate (see Fig. 2) shows a ∼25% reduction centered at the primary eclipse (orbital phase 1.0) with the dip confined to totality. We have not observed any count rate dips at secondary eclipses, but this could be due to the flaring state of the source during all the annular eclipses we observed (Nov 2, Nov 4, and Nov 12).

In Fig. 1 we also plot the PDS light curve binned over 3600 sec. About a half of the PDS data are upper limits. The PDS count rates oscillate around 0 with a standard deviation of 0.15 and 0.13 cts s^{-1} in the two observing runs, respectively. Several sporadic increases of the hard X-ray flux were observed exceeding $1\,\sigma$, but not apparently correlated with the soft X-ray flux behaviour. However, the two following cases could be exceptions: *i)* on Nov 4, at the end of the 1st observing run, the increase in the PDS count rate exceedes $3\,\sigma$ and appears to be coincident with the soft X-ray flare observed by the MECS at ∼15:40 UT (see also Fig. 2 at phase 1.6); *ii)* on Nov 11, during the major soft X-ray flare oberved by the MECS and LECS, the hard X-ray flux appears to be decaying exponentially from a greater than $2\,\sigma$ initial value.

3.2. The X-ray spectra

The spectra from the LECS and from the MECS detectors were analysed using an optically-thin plasma emission model with two discrete temperature components and variable global metal abundances (the abundances of individual elements have the same ratios as in the solar case). In fact, the limited spectral resolution of LECS and MECS does not permit a reliable determination of coronal abundances of individual elements. The

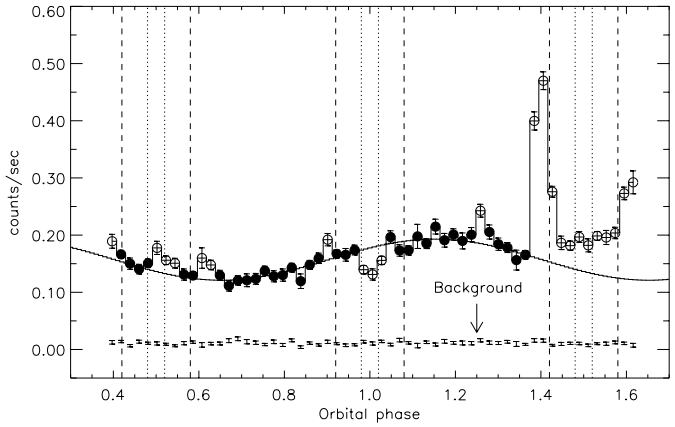

Fig. 2. SAX MECS (1.7–10 keV) AR Lac light curve and background binned over 3600 sec and folded with the orbital period. No data points are repeated. Error bars indicate $\pm 1\,\sigma$ deviations. The 1st and 4th contacts of the photosphere eclipses are drawn with vertical dashed lines, and the 2nd and 3th contacts are drawn with dotted lines. Phases have been computed by using the ephemeris HJD=2450692.5174+1.983188xE (Marino et al. 1998).

MEKAL code under XSPEC 10.0, based on the model of Mewe and Kaastra with Fe L calculations by Liedahl (Mewe et al. 1995), was used for this analysis. The assumed solar abundances are those of Anders & Grevesse (1989). The effect of interstellar absorption was taken into account using the model of Morrison & McCammon (1983) as in the XSPEC-WABS code. Taking into account a neutral hydrogen volume density of 0.07 cm^{-3} (Paresce 1984) and the distance d=42 pc measured by H IPPARCOS (Perryman et al. 1997), the neutral hydrogen column density would amount to $N_H \sim 10^{19}$ cm^{-2}. However, this is an approximate value because the H I extintion is inhomogeneous. Walter (1996) and Griffiths & Jordan (1998) estimated a much lower value of $N_H \sim 2\times10^{18}$ cm^{-2}, using the ratio between the Fe XVI lines at 335 and 361 Å as observed by EUVE. Linsky et al. (1998) estimated in the direction of AR Lac N_H=(5.9±2.5)$\times10^{18}$ cm^{-2} by interpolating measurements of the H I extintion in directions closeby to AR Lac in the local interstellar cloud.

In our spectral fits we first fixed N_H to the value derived by Linsky et al. (1998), and then allowed it to vary to derive the best-fit N_H value. Freezing N_H to 5.9×10^{18} cm^{-2}, and contemporarly fitting together the total LECS and MECS spectra (T) we derived the best-fit model spectrum and the fit residuals shown in Fig. 3. The fit has a reduced χ^2 of 1.06 with 358 degree of freedom (d.o.f). The best fit temperatures are 2.05±0.07 keV and 0.77±0.03 keV, with a ratio between the two emission measures (cool/hot) of 0.58 (EM_{cool}=1.82×10^{53} cm^{-3} and EM_{hot}=3.13×10^{53} cm^{-3}). The global metal abundance is 0.66±0.06. The reduced χ^2 of this best-fit is acceptable, but the fit is poor below 0.25 keV and in the region of the Fe complex at 6.7 keV. The best-fit rescaling factor is ∼0.7 for the LECS to the MECS. The best-fit parameters are given in Table 2.

We then performed the analysis with N_H as a free parameter, and obtained the best-fit model spectrum and the fit residuals shown in Fig. 4 (see Table 3). The fit has a better reduced χ^2 of 0.95 (with 357 d.o.f). The resulting best fit temperatures do not change appreciably, but the ratio between the cool/hot emission measures increases to 0.95 and the global metal abundance decreases to 0.43±0.02. The N_H value resulted even higher than expected, $(6.1\pm1.5)\times10^{19}$ cm^{-2}.

It is well known that high values of interstellar absorption can mimic low metallicity (Tagliaferri et al. 1997). Moreover, lower best-fit metallicities are known to be correlated with higher emission measure ratios between the cool and the hot components (Favata et al. 1997a). A low metal abundance (0.33) also results from analyzing MECS data using the MEKAL model without interstellar absorption, since the interstellar absorption is negligible at energies above 1.8 keV. On the other hand, since the metal abundances are measured by the relative intensity between emission lines and continuum, the abundances inferred by analysing only the MECS data could be in error because of the lack of line-free continuum flux in the energy range covered by the MECS. The presence of a strong and systematic dependence of the best-fit metallicity on the spectral region being fitted was also pointed out by Favata et al. (1997a), who applied two component MEKAL plasma models on both simulated and real spectra of Beppo-SAX LECS and ASCA SIS instruments.

The spectral analysis of the two separate segments of observations (Nov 2–4, and Nov 11–12) was done with N_H constrained to 5.9×10^{18} cm^{-2}. We found that the two-component temperatures did not significantly change between the two time intervals (see Table 2). On the contrary, the best-fit global metal abundance seems to be slightly variable. We note, however, that the higher global metal abundance resulting from the 2nd observation could be linked to the low integration time for the Fe K line complex at 6.7 keV and the resulting poorer statistics in the 2nd run MECS spectrum. We therefore conclude that there is no evidence in these data for temporal variability of the coronal metal abundance of AR Lac.

It is worth noting that we were not able to reproduce very well the Fe K line complex region around ∼6.7 keV. The fit of the Fe K feature is bad both when we model the total 0.1–10 keV spectrum, and when we model the MECS spectrum only. Conversely, the spectral line seems to be narrower than expected from the model. We checked for possible calibration problems or other effects linked to the detector by discussing these questions with people on the MECS team at the IFCAI-CNR (Palermo), and we had to conclude that the observed feature should be real. A slight deficiency of the model near the Fe-K complex above 6 keV was also reported by Kaastra et al. (1996) who analyzed AR Lac ASCA spectra with the SPEX plasma model.

In order to improve our fit in the 6.7 keV region, we also let the Fe abundance to vary separately from the other elements, but we immediately faced the problem that, given the available spectral resolution, the individual element abundances cannot be constrained with sufficient confidence.

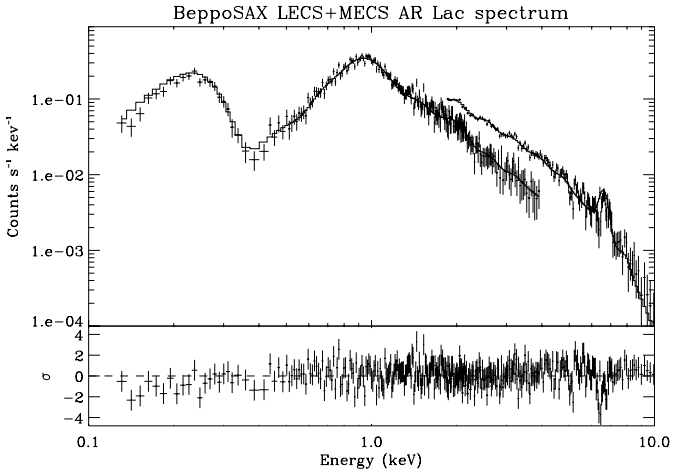

Fig. 3. SAX LECS+MECS total spectrum (T), together with the best fit two temperature MEKAL model spectrum plus the interstellar absorption component (WABS code). The neutral hydrogen column density N_H was fixed to 5.9×10^{18} cm^{-2} (Linsky et al. 1998).

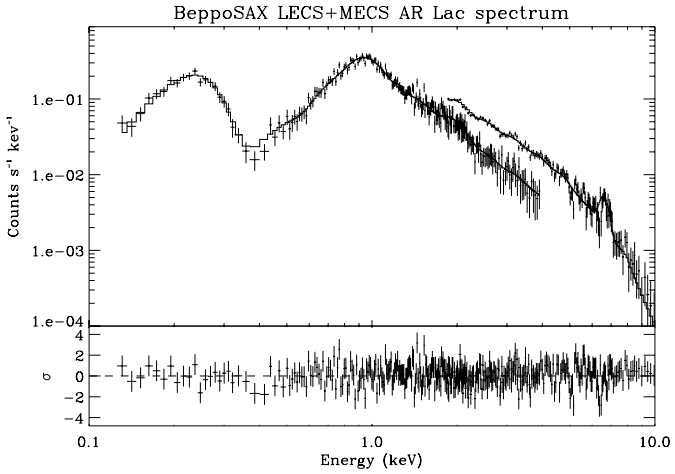

Fig. 4. As in Fig. 3, but the neutral hydrogen interstellar column density N_H was taken as a free parameter in the fitting procedure.

Since the Fe abundance was observed to be variable with the state, quiescent or flaring, of the source (see Stern et al. 1992, White, Pallavicini, & Lim 1995, Mewe et al. 1997 and Güdel et al. 1999), we have searched for a better fit of the Fe K line complex also by allowing the global metal abundance to be different for the two plasma components. Assuming N_H=5.9×10^{18} cm^{-2}, we found a solution with a reduced χ^2 of 0.97 (357 d.o.f.) that implies almost the same temperatures reported before, an abundance of 0.40 solar for the hot component, and a super-solar abundance of 1.94 solar for the cool component, with an emission measure ratio of 0.17 between the cool and the hot components. However, the cool component abundance is not very well constrained; it can be between 1.17–6.71 (90% confidence level). Moreover, the Fe K line complex is not better fit by this model. Therefore, we cast doubt on the physical significance of this solution.

We also attempted to fit the data with a three-temperature MEKAL model, but we did not find a significant improvement by adding a third component, either of intermediate or of higher temperature (the instruments are sensitive for temperatures in the range $\sim$0.1–10 keV).

4. Discussion

The AR Lac light curve observed by the Beppo SAX MECS shows a very narrow primary eclipse and no signature of a secondary eclipse. However, at the times of the three observed secondary eclipses, the system apparently was in a low-level flaring state which could have filled-in any small secondary eclipse dip. During the primary eclipse the reduction in the MECS count rate was $\sim$25%, which is comparable to the $\sim$32% decrease observed by the *Einstein* IPC (Walter et al. 1983), but less than the $\sim$45%, $\sim$40%, and $\sim$50% decreases observed by the EXOSAT LEIT (White et al. 1990), ROSAT PSPC (Ottmann et al. 1993), and ASCA GIS&SIS (White et al. 1994), respectively. Such a comparison is justified, because even though the MECS is not very sensitive at the low energies ($<$1.7 keV), no strong energy dependence of the overall orbital modulation was found by the above quoted ROSAT PSPC and ASCA observations, with the depth of the primary eclipse above 2 keV similar to that at low energies. The important aspect of our Beppo-SAX observations is the short duration of the primary eclipse that seems to begin after the 2nd contact and to end before the 4th contact. Such a short eclipse, indicates a well localized and confined G-star corona. Similar but somewhat longer primary eclipses were observed by the *Einstein* IPC (Walter et al. 1983) and ROSAT PSPC (Ottmann et al. 1993), while the primary ecplises observed by EXOSAT and ASCA (White et al. 1990, White et al. 1994) were much larger with gradual ingress and egress extending well before and after the 1st and 4th contacts, respectively. Moreover, we recall that no primary eclipse at all was observed by the EXOSAT ME (1–6 keV) detector (White et al. 1990), and that this was interpreted as due to the high temperature component of the X-ray plasma being extended on a scale comparable to the binary separation. The scenario that can be drawn from the comparison of the results of all of the available X-ray observations of AR Lac is that the spatial structure of the corona of this system varies with time.

Our analysis of the AR Lac X-ray spectra confirms the existence of a bimodal temperature structure, with the cool component at about 0.8 keV and the hot at about 2.0 keV, consistent with the results of White et al. (1994) and Kaastra et al. (1996), based on the analysis of ASCA data, and of Walter (1996) who analyzed EUVE data. The MECS light curve gives essential information on the high temperature component, that seems to be very well confined and localized close to the G star at the time of our Beppo-SAX observations. No observations were made with the LECS detector during primary eclipses, so we cannot infer anything about the localization of the low temperature component.

Our data confirm that the metal abundances of the AR Lac corona are different from those of the solar photosphere. We obtain a global metal abundance, Z=0.65 solar, that is a bit less

Table 2. Results of a two-components MEKAL plasma model fit to the spectral data. The neutral hydrogen interstellar column density N_H was fixed to to 5.9×10^{18} cm^{-2} (Linsky et al. 1998).

Run	χ^2	dof	Z	90% conf. range	T_c (keV)	90% conf. range	$EM_c/10^{53}$ cm^{-3}	T_h (keV)	90% conf. range	$EM_h/10^{53}$ cm^{-3}	$\frac{EM_c}{EM_h}$	$f_x/10^{-11}$ erg cm^{-2} s^{-1}
1	1.23	300	0.57	0.51–0.65	0.80	0.76–0.83	2.3	2.11	2.02–2.23	3.1	0.73	2.75
2	1.07	242	0.73	0.63–0.85	0.76	0.71–0.80	1.7	2.01	1.91–2.13	2.9	0.57	2.77
Total	1.04	359	0.65	0.58–0.72	0.78	0.74–0.81	1.8	2.06	1.98–2.14	3.1	0.58	2.82

Table 3. Results of a two-components MEKAL plasma model fit to the total spectral data (T). The neutral hydrogen interstellar column density N_H was left free to vary in the fit procedure.

N_H 10^{19} cm^{-2}	χ^2	dof	Z	90% conf. range	T_c (keV)	90% conf. range	$EM_c/10^{53}$ cm^{-3}	T_h (keV)	90% conf. range	$EM_h/10^{53}$ cm^{-3}	$\frac{EM_c}{EM_h}$	$f_x/10^{-11}$ erg cm^{-2} s^{-1}
6.6	0.95	364	0.41	0.40–0.42	0.81	0.79–0.82	3.1	2.21	2.18–2.25	3.1	0.99	2.72

than twice the mean value claimed by White et al. (1994) and by Kaastra et al. (1996), who constrained the individual element abundances using ASCA data, and by Walter (1996), who estimated a $\frac{Fe}{H}$ ratio equal to 0.39 solar from EUVE spectra. However, we found that a coronal plasma with a global metal abundance of 0.41 could adequately reproduce also the Beppo-SAX spectra if one let the neutral hydrogen column density be about 10 times higher than expected by Linsky et al. (1998). Conversely, the data in the region below 0.5 keV could not be fitted with the low global metal abundance that best fit the data at high energy, unless one assumes a much larger H I interstellar absorption than is implied by HST observations along nearby lines of sight. It is worth noting that the ASCA instruments are not sensitive under 0.5 keV, therefore the ASCA data cannot lead to a similar result. In at least two other cases - VY Ari (Favata et al. 1997b) and HD 9770 (Tagliaferri et al. 1997) - the Beppo-SAX LECS data could be fitted best by assuming a higher than expected H I column density. We now pose the question if the extra-absorption required by the AR Lac Beppo-SAX spectrum below 0.5 keV can be due to circumstellar H I or to H I in the stellar corona. From Hα observations of AR Lac obtained in 1997, Frasca et al. (1999) found evidence of circumstellar material before and during the primary eclipse. Moreover, recent data on Sun, e.g. TRACE data (Hurlburt et al. 1998), showed the presence of bound-free absorption due to H I in the solar coronae. If the solar-stellar analogy is valid also in this context, not to take into account the H I bound-free absorption in the stellar corona, could be reflected in a large value of the H I interstellar column density, as it results from our best-fit of the AR Lac X-ray spectrum.

Our analysis of the AR Lac Beppo-SAX data emphasize the dependence of derived abundances on the precise spectral quantity being fit and the mutual interdependence of N_H, Z and the two component emission measure ratios. This result lead us to question the credibility of the abundance values that are found when analyzing stellar coronae. Drake (1998) suggested as alternative explanation for the apparently low metal abundances observed in some stellar coronae, that the He abundance in these coronae is enhanced (e.g. doubled), causing lower line-to-continuum ratios. The He might be selectively enhanced by preferential mechanisms for retention of He nuclei in the corona or by diffusion processes. Conversely, we performed a spectral analysis using a two component MEKAL plasma model with all element abundances fixed equal to those of the solar photosphere, except for He which was left as a free parameter in the fitting procedure, and found that an acceptable solution (χ^2=1.07, 351 d.o.f.) can be found for a He abundance of 2.6$\pm$0.5 times the solar photospheric value, and a temperature structure that is almost the same as in the case of a metal deficient plasma (T_c $\sim$0.78 keV, T_h $\sim$2.05 keV and EM_c/EM_h $\sim$0.59). If the He abundance is really enhanced or if the stellar coronae are really metal poor is a topic that will be probably best addressed only by the more sensitive and with better spectral resolution future X-ray missions.

Acknowledgements. Research on stellar activity at Catania University and Astrophysical Observatory is supported by MURST (*Ministero dell'Università e della Ricerca Scientifica e Tecnologica*). This research has made use of SAXDAS linearized and cleaned event files (Rev.1.1) produced at the Beppo-SAX Science Data Center. We would thanks L. Chiappetti G. Cusumano and G. Tagliaferri for useful and precious suggestions and discussions, and J.L. Linsky for his comments and suggestions. We are also indebted with A. Antonelli and F. Fiore of Beppo-SAX Science Data Center for having helped us in data reduction. Finally, we would extend our thanks to HEASARC people for the support they give with FTOOLS and XANADU software.

References

Anders E., Grevesse N., 1989, Geochim. Cosmochim. Acta 53, 197
Arnaud K.A., 1996, In: Jacoby G., Barnes J. (eds.) Astronomical Data Analysis Software and Systems V. ASP Conf. Ser. Vol. 101, p. 17
Boella G., Butler R.G., Perola G.C., et al., 1997a, A&AS 122, 299
Boella G., Chiappetti L., Conti G., et al., 1997b, A&AS 122, 327

Dempsey R.C., Linsky J.L., Schmitt J.H.M.M., Fleming T.A., 1993, ApJ 413, 333
Drake J.J., 1998, ApJ 496, L33
Favata F., Maggio A., Peres G., Sciortino S., 1997a, A&A 326, 1013
Favata F., Mineo T., Parmar A.N., Cusumano G., 1997b, A&A 324, L41
Frasca A., Marino G., Catalano S., Marilli E., 1999, private communication
Frontera F., Costa E., Dal Fiume D., et al., 1997, A&AS 122, 357
Griffiths N.W., Jordan C., 1998, ApJ 497, 428
Güdel M., Linsky J.L., Brown A., Nagase F., 1999, ApJ 511, 405
Hurlburt N., Schijver C., Shine R., Tarbell T., Title A., 1998, In: 1998 Fall Meeting of the American Geophysical Union. AGU Vol. 79, N45
Kaastra J.S., Mewe R., Liedahl D.A., et al., 1996, A&A 314, 547
Lanza A.F., Catalano S., Cutispoto G., Pagano I., Rodonò M., 1998, A&A 332, 541
Linsky J.L., 1988, In: Córdova F. (ed.) Multiwavelength Astrophysics. Cambridge, p. 49
Linsky J.L., Piskunov N., Wood B.E., 1998, in preparation
Majer P., Schmitt J.H.M.M., Golub L., Harnden Jr. F.R., Rosner R., 1986, ApJ 300, 360
Marino G., Catalano S., Frasca A., Marilli E., 1998, IBVS 4599
Mewe R., Kaastra J.S., Liedahl D.A., 1995, Legacy 6, 16
Mewe R., Kaastra J.S., White S.M., Pallavicini R., 1996, A&A 315, 170
Mewe R., Kaastra J.S., van den Oord G.H.J., Vink J., Tawara Y., 1997, A&A 320, 147
Morrison R., McCammon D., 1983, ApJ 270, 119
Neff J.E., Walter F.M., Rodonò M., Linsky J.L., 1989, A&A 215, 79
Naftilan S.A., Drake S.A., 1977, ApJ 216, 508
Ottmann R., Schmitt J.H.M.M., Kürster M., 1993, ApJ 413, 710
Pagano I., 1994, Ph.D. Thesis, Catania University
Pagano I., Rodonò M., Neff J.E., Walter F.M., 1994, In: Caillault J.P. (ed.) The VIII Cambridge Workshop on Cool Stars, Stellar Systems and the Sun. ASP Conf. Ser. Vol. 64, 450
Pagano I., Rodonò M., Walter F.M., Neff J.E., 1995, In: Uchida Y., Kosugi T., Hudson H.S. (eds.) Magnetodynamic Phenomena in the Solar Atmosphere – Prototypes of Stellar Activity. IAU Coll. 153, Kluwer Ac. Pub., p. 631
Paresce F., 1984, AJ 89, 1022
Parmar A.N., Martin D.D.E., Bavdaz M., et al., 1997, A&AS 122, 309
Perryman M.A.C., The HYPPARCOS Science Team, 1997, ESA SP-1200, Vol.1–12, ESA Publication division, c/o ESTEC, Noordwijk, The Netherlands
Randich S., Giampapa M.S., Pallavicini R., 1994, A&A 283, 893
Rodonò M., 1982, In: Achievements in Stellar Astrophysics. Adv. Space Res. 2, No. 9, 225
Siarkowski M., Pres P., Drake S.A., White N.E., Singh K.P., 1996, ApJ 473, 470
Stern R.A., Uchida Y., Tsuneta S., Nagase F., 1992, ApJ 400, 321
Swank J.H., White N.E., Holt S.S., Becker R.H., 1981, ApJ 246, 208
Swank J.H., White N.E., 1980, In: Dupree A.K. (ed.) Cool Stars, Stellar Systems and the Sun. Cambridge: Smithsonian Astrophys. Obs., Special Report 389, p. 47
Tagliaferri G., Covino S., Cutispoto G., Pallavicini R., 1997, Proc. of The Active X-Ray Sky, Palermo Astronomical Observatory Preprint N. 4/98
Walter F.M., 1996, In: Bowyer S., Malina R.F. (eds.) Astrophysics in Extreme Ultraviolet. IAU Coll. 152, Kluwer Ac. Pub., p. 129
Walter F.M., Gibson D.M., Basri G.S., 1983, ApJ 267, 665
Walter F.M., Neff J.E., Gibson D.M., Linsky J.L., Rodonò, M., 1987, A&A 186, 241
White N.E., Shafer R.A., Horne K., Parmar A.N., Culhane J.L., 1990, ApJ 350, 776
White N.E., Arnaud K., Day C.R.S, et al., 1994, PASJ 46, L97
White N.E., Pallavicini R., Lim J., 1995, In: Greiner J., Duerbeck H.W., Gershberg R.E. (eds.) Flares and Flashes. Proc. IAU Coll 151, Springer, Berlin, p. 168